

Entropic effects on the Size Evolution of Cluster Structure

Jonathan P. K. Doye and Florent Calvo[†]

University Chemical Laboratory, Lensfield Road, Cambridge CB2 1EW, United Kingdom

We show that the vibrational entropy can play a crucial role in determining the equilibrium structure of clusters by constructing structural phase diagrams showing how the structure depends upon both size and temperature. These phase diagrams are obtained for example rare gas and metal clusters.

PACS numbers: 61.46.+w, 36.40.Mr, 36.40.Ei

Much of the interest in clusters or nanoparticles derives from the insights they can provide into how properties emerge and evolve on going between the atomic and molecular and bulk limits. Cluster structure provides a particular interesting example of this size evolution. At large enough sizes the clusters must display the bulk crystalline structure, but this limit may sometimes only be achieved at very large sizes (e.g. at least 20 000 atoms for sodium clusters [1]) and before that limit is reached unusual structural forms are often observed. For example, many clusters bound by van der Waals or metallic forces exhibit structures with five-fold axes of symmetry, a possibility that is forbidden in bulk crystalline materials. For these clusters the dominant structural motif typically changes from icosahedral (Fig. 1(b)) to decahedral (Fig. 1(c)) to face-centred-cubic (fcc) (Fig. 1(a)) as the size increases.

For many materials these structural changes occur at sizes that are too large for global optimization to be feasible. Therefore, the typical theoretical approach to systematically investigating the size evolution of cluster structure is to compare the energies of stable sequences of structures, such as the forms shown in Fig. 1. ‘Crossover sizes’ are then identified where the sequence with lowest energy changes. At this crossover the most common equilibrium structure is expected to change. This technique has been applied to rare gas [2, 3, 4], metal [5, 6, 7, 8] and molecular clusters [9].

The above approach is certainly valid at zero temperature, since the equilibrium structure then corresponds to the one with lowest energy. At other temperatures, however, the structure with lowest free energy needs to be found. However, perhaps through an expectation that entropic effects are unlikely to be important or are too complicated to take into account, size is usually the only variable that is considered both experimentally [10, 11, 12] and theoretically [2, 3, 4, 5, 6, 7, 8].

In this paper we consider the role that entropy plays in the size evolution of cluster structure, and show that temperature can be a key variable in determining the equi-

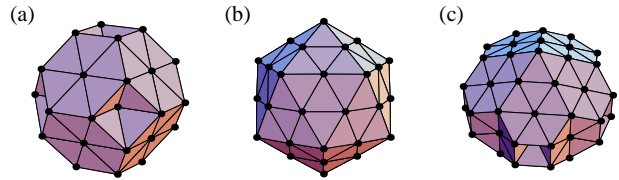


FIG. 1: Three examples of the structures clusters can adopt: (a) a fcc 38-atom truncated octahedron, (b) a 55-atom Mackay icosahedron [13], and (c) a 75-atom Marks decahedron [14]. These clusters have the optimal shape for the three main types of regular packing seen in clusters: face-centred cubic, icosahedral and decahedral, respectively. The latter two structural types cannot be extended to bulk because of the five-fold axes of symmetry.

librium structure of a cluster. A clue to this result can be garnered from the growing number of examples of solid-solid transitions in clusters where the structure changes from fcc or decahedral to icosahedral as the temperature increases [15, 16, 17, 18, 19]. The most well-investigated examples of these transitions are for those small Lennard-Jones (LJ) clusters that have a non-icosahedral global minimum. For $N < 150$ there are only 8 examples and these occur at sizes where the non-icosahedral morphology has a near optimum shape, whereas the icosahedral structures have an incomplete outer layer. The global minimum is fcc at $N=38$, decahedral at $N=75-77, 102-104$ and has an unusual structure called a Leary tetrahedron at $N=98$ [20].

Here we analyse these examples further in order to identify what is the most significant contribution to the difference in entropies between the structural types, particularly as the size increases. Direct computation of T_{ss} , the temperature of the solid-solid transition, is possible by parallel tempering [21], but this is computationally demanding because of the large (free) energy barriers between the structural types [17, 22], and has only been done for LJ₃₈ [23].

TABLE I: Estimates of the solid-solid transition temperature T_{ss} for those Lennard-Jones clusters with less than 150 atoms that have non-icosahedral global minima. $\bar{\nu}_A$ and $\bar{\nu}_B$ are the mean frequencies of the lowest-energy non-icosahedral and icosahedral minima, respectively. ϵ is the equilibrium pair well depth of the LJ potential.

N	$T_{ss}/\epsilon k^{-1}$				
	HSM	Einstein	Eq. (3)	$\Delta E/\epsilon$	$\bar{\nu}_A/\bar{\nu}_B$
38	0.121	0.199	0.316	0.676	1.0200
75	0.082	0.234	0.119	1.210	1.0475
76	0.046	0.223	0.053	0.510	1.0446
77	0.048	0.199	0.057	0.565	1.0451
98	0.004	0.009	0.006	0.022	1.0135
102	0.013	0.096	0.014	0.086	1.0201
103	0.016	0.116	0.018	0.107	1.0204
104	0.007	0.069	0.008	0.048	1.0212

The superposition method [24, 25] provides another approach to this calculation and one which is particularly useful for our present purposes because it allows us to analyse the different contributions to the entropy. In this approach the partition function is written as a sum over all the minima on the potential energy surface, and by restricting the sum to a certain subset of the minima the thermodynamic properties of a particular region of configuration space can be obtained. The centre of the solid-solid transition occurs when the partition functions for the two competing structural types are equal, i.e. $Z_A = Z_B$. In the harmonic approximation [26] this then gives

$$\sum_{i \in A} \frac{n_i \exp(-\beta E_i)}{\bar{\nu}_i^{3N-6}} = \sum_{j \in B} \frac{n_j \exp(-\beta E_j)}{\bar{\nu}_j^{3N-6}}, \quad (1)$$

where $\beta=1/kT$, E_i is the potential energy of minimum i , $\bar{\nu}_i$ is the geometric mean vibrational frequency, and $n_i=2N!/h_i$ is the number of permutational isomers of i , where h_i is the order of the point group. T_{ss} values calculated using Eq. (1) are given in Table I. It is noteworthy that there is a general decrease in the values with increasing size.

One contribution to the entropy of a morphology comes from the number of low-energy minima of that type. For the current examples this term always favours the icosahedra because there are many low-energy icosahedral minima with different arrangements of the atoms in the incomplete outer layer [22]. Another entropic contribution can come from the symmetry of the cluster. At $N=38, 75$ and 98 the global minimum has high symmetry, thus reducing the number of permutational isomers. For these three sizes this factor again favours the icosahedra. Lastly, there is the vibrational entropy. For the current examples the icosahedral structures have a smaller mean vibrational frequency, which again favours

the icosahedra. However, unlike the previous two contributions to the entropy, this term favours the icosahedra for a LJ cluster of any size. Furthermore, the absence of any solid-solid transitions when the LJ global minimum is icosahedral therefore suggests that the vibrational entropy is crucial.

We can analyse further the effect of the vibrational entropy by applying an Einstein approximation, i.e. we assume that all the minima have the same mean vibrational frequency. The resulting values for T_{ss} are also given in Table I. Although the transitions still occur, they do so at significantly higher temperature with the error increasing with size, because $\bar{\nu}$ is raised to the power $3N-6$ in Eq. (1). This increasing dominance of the vibrational entropy is the main reason that the actual T_{ss} generally decrease with size. These results, therefore, suggest that solid-solid transitions, rather than being unusual, should be expected for systems where different structural types have systematic differences in $\bar{\nu}$ at sizes where the morphology with lower vibrational entropy is the lowest in energy.

To obtain our results for T_{ss} we systematically searched the low-energy regions of the potential energy surface for these clusters in order to generate the relevant samples of low-energy minima. However, this is not a practical approach at large sizes, therefore we seek a simpler way to estimate T_{ss} . Firstly, if we assume that all the minima associated with a morphology have the same energy and vibrational frequency, then

$$T_{ss} = \frac{\Delta E}{k(\log(n_B/n_A) + (3N-6)\log(\bar{\nu}_A/\bar{\nu}_B))}, \quad (2)$$

where $\Delta E=E_B-E_A$ and n_A is the total number of minima (geometric and permutational isomers) associated with morphology A. Although in all the specific examples in Table I there are far more icosahedral low-energy minima, on average the number of minima will be approximately the same. Furthermore, at large sizes the vibrational term will dominate the denominator. In this limit

$$T_{ss} = \frac{\Delta E}{k(3N-6)\log(\bar{\nu}_A/\bar{\nu}_B)} \quad (3)$$

We tested this expression for the examples in Table I using the properties of the lowest-energy minima of the two competing morphologies. As expected this estimate becomes more accurate as the size increases, and the errors for the largest sizes are small.

We can also use Eq. (3) to determine how crossover sizes depend on temperature. As with the theoretical studies mentioned earlier, we can compare stable sequences of structures, but now monitoring not only their energies but also their vibrational frequencies. These properties can be fitted to the forms

$$E = a_E N + b_E N^{2/3} + c_E N^{1/3} + d_E \quad (4)$$

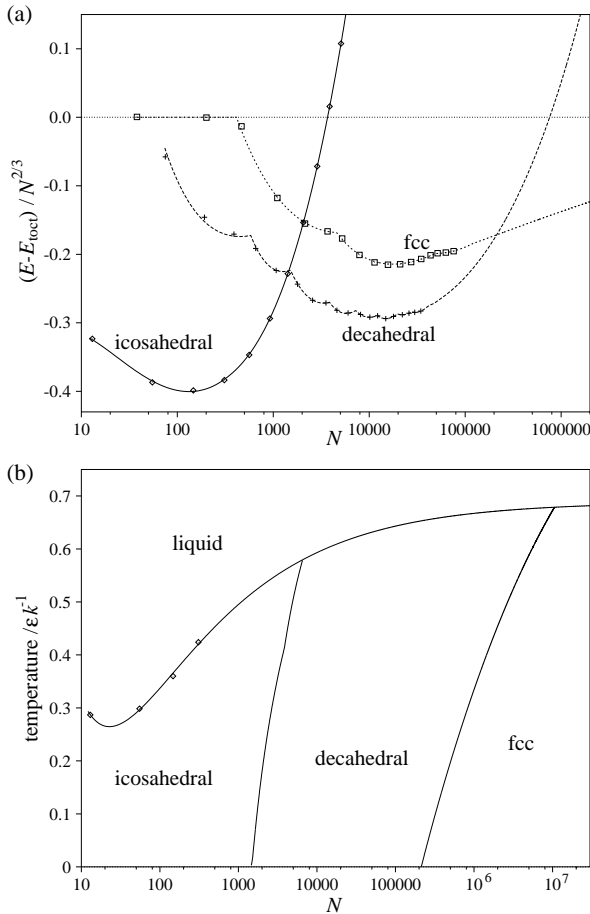


FIG. 2: (a) Energies of the competing structural types for LJ clusters. The data points represent clusters with the optimal shape at that size, and the continuous lines are fits to these data using Eq. (4). The energy zero is E_{toct} , a fit to the fcc truncated octahedra with regular hexagonal {111} faces (Fig. 1(a)). (b) Structural phase diagram for LJ clusters. The data points represent the melting temperatures of the four smallest Mackay icosahedra. For argon $1\epsilon k^{-1} \equiv 121\text{K}$.

$$\bar{\nu} = a_\nu + \frac{b_\nu}{N^{1/3}} + \frac{c_\nu}{N^{2/3}} + \frac{d_\nu}{N} \quad (5)$$

where the first two terms represent volume and surface contributions, respectively. These expressions can then be input into Eq. (3) to map out the solid-solid transitions in the structural phase diagram. Finally to complete the diagram, the melting line has to be determined. Again it will have the form

$$T_m = a_m + \frac{b_m}{N^{1/3}} + \frac{c_m}{N^{2/3}} + \frac{d_m}{N}. \quad (6)$$

We first present results for LJ clusters, which provide a reasonable model of heavy rare gas clusters, such as argon. Up to $N \approx 10\,000$ the energies of the stable sequences of structures were obtained by minimization of all degrees

of freedom. Above this size minimizations were possible up to $N \approx 35\,000$ for decahedral and $N \approx 80\,000$ for fcc structures if the cluster was constrained to maintain the correct point group symmetry (D_{5h} for decahedral and O_h for fcc). The energies of the optimal clusters for each structural type are shown in Fig. 2(a). The lobed shape of the decahedral and fcc lines results from changes in the shape of the optimal sequence; as the size increases the forms depicted in Fig. 1(a) and (c) become more rounded by the introduction of {110} facets of increasing size, and the grooves in the Marks decahedra become deeper. The energetic crossover sizes are consistent with previous results [4]: $N_{\text{icos} \rightarrow \text{deca}}(T=0) \approx 1450$ and $N_{\text{deca} \rightarrow \text{fcc}}(T=0) \approx 213\,000$.

In order to calculate $\bar{\nu}$ the Hessian matrix must be diagonalized, and so the sizes for which $\bar{\nu}$ can be calculated are limited to $N < 3500$. Above this size we rely upon the extrapolation of Eq. (5). To construct the melting line a_m is assigned the value of the zero pressure bulk melting temperature [27] and the other three parameters in Eq. (6) are fitted using the melting points of the first four Mackay icosahedra, which were obtained from Monte Carlo simulations.

The structural phase diagram that results from these calculations is shown in Fig. 2(b). When interpreting these diagrams, one should remember that the phase boundaries divide the plane into regions where the majority of clusters have a particular equilibrium structure. If the non-monotonic variation of cluster properties, as illustrated by the examples in Table I, were fully taken into account, the phase boundaries would be considerably rougher.

The effect of the vibrational entropy can be clearly seen from the slopes of the phase boundaries in Fig. 2(b), e.g. $N_{\text{icos} \rightarrow \text{deca}}(T_m) \approx 6550$ and $N_{\text{deca} \rightarrow \text{fcc}}(T_m) \approx 10\,600\,000$. At higher temperatures icosahedra and Marks decahedra remain most stable up to considerably larger sizes. This is because of the relative values of their vibrational frequencies: a_ν^{icos} and a_ν^{deca} are 2.06% and 0.19% less than a_ν^{fcc} , respectively. Even though the difference between fcc and decahedral frequencies is much smaller, the effect on the slope of the phase boundary is larger because of the larger value of N in the denominator of Eq. (3).

The techniques that we have developed are readily applicable to other atomic clusters. This is illustrated in Fig. 3 for silver clusters described by the Sutton-Chen potential [28]. The phase diagram has a very similar form to the LJ diagram except that the crossovers occur at smaller sizes, and again the icosahedra and decahedra are substantially stabilized by temperature. $N_{\text{icos} \rightarrow \text{deca}}(0) \approx 240$ and $N_{\text{deca} \rightarrow \text{fcc}}(0) \approx 36\,600$ compared to $N_{\text{icos} \rightarrow \text{deca}}(T_m) \approx 3500$ and $N_{\text{deca} \rightarrow \text{fcc}}(T_m) \approx 253\,000$.

However, the method cannot be simply applied to molecular clusters because the orientational degrees of freedom add an extra degree of complexity. Tests on

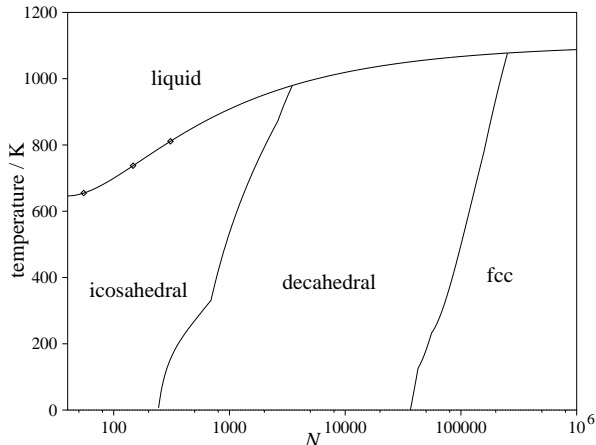


FIG. 3: Structural phase diagram for silver clusters.

N_2 clusters showed that for minima where the molecular centres have a common structure but the molecules have different orientations there is a considerable variation in $\bar{\nu}$. Thus one of the assumptions underlying the use of Eq. (3) is invalidated and one would have to consider the competition between orientational isomers as well as between structural types.

The key role that we have shown the temperature to play in determining the equilibrium structure of a cluster underlines the importance of only comparing clusters that have both the same size and temperature. This may help to explain some of the apparent contradictions between experiments and zero-temperature theoretical calculations and between different experiments (e.g. electron diffraction [10] and EXAFS [11] predict different crossover sizes for rare gas clusters).

Although the developments in this paper allow a more complete comparison of theory and experiment, it should be remembered that equilibrium may be hard to achieve in experiment. For example, experiments on gold clusters [29] and clusters of C_{60} molecules [30] show the importance of annealing the clusters at sufficiently high temperature to locate the most stable forms. Furthermore, the (free) energy barriers between structural types [17, 22], which have been shown to be large for LJ clusters, are likely to increase with size, making structural transformations increasingly hard. In such a situation, growth may preserve the dominant structure at the last size at which equilibrium was obtained [31], or may occur around a core structure that allows rapid growth [32].

JKPD is grateful to Emmanuel College, Cambridge for financial support, and FC has been supported by a European Community Marie Curie Fellowship.

[†] Permanent address: Laboratoire de Physique Quantique, IRSAMC, Université Paul Sabatier, 118 Route de Narbonne, F31062 Toulouse Cedex.

- [1] T. P. Martin, T. Bergmann, H. Göhlich, and T. Lange, *Chem. Phys. Lett.* **172**, 209 (1990).
- [2] J. Xie, J. A. Northby, D. L. Freeman, and J. D. Doll, *J. Chem. Phys.* **91**, 612 (1989).
- [3] B. W. van de Waal, *J. Chem. Phys.* **90**, 3407 (1989).
- [4] B. Raoult, J. Farges, M.-F. de Feraudy, and G. Torchet, *Phil. Mag. B* **60**, 881 (1989).
- [5] C. L. Cleveland and U. Landman, *J. Chem. Phys.* **94**, 7376 (1991).
- [6] H. S. Lim, C. K. Ong, and F. Ercolelli, *Surf. Sci.* **269/270**, 1109 (1992).
- [7] C. L. Cleveland *et al.*, *Phys. Rev. Lett.* **79**, 1873 (1997).
- [8] C. Barreteau, M. C. Desjonquères, and D. Spanjaard, *Eur. Phys. J. D* **11**, 395 (2000).
- [9] F. Calvo, G. Torchet, and M.-F. de Feraudy, *J. Chem. Phys.* **111**, 4650 (1999).
- [10] J. Farges, M.-F. de Feraudy, B. Raoult, and G. Torchet, *Adv. Chem. Phys.* **70**, 45 (1988).
- [11] S. Kakar *et al.*, *Phys. Rev. Lett.* **78**, 1675 (1997).
- [12] G. Torchet, M.-F. de Feraudy, A. Boutin, and A. H. Fuchs, *J. Chem. Phys.* **105**, 3671 (1996).
- [13] A. L. Mackay, *Acta Cryst.* **15**, 916 (1962).
- [14] L. D. Marks, *Phil. Mag. A* **49**, 81 (1984).
- [15] J. P. K. Doye, D. J. Wales, and R. S. Berry, *J. Chem. Phys.* **103**, 4234 (1995).
- [16] J. P. K. Doye and D. J. Wales, *Phys. Rev. Lett.* **80**, 1357 (1998).
- [17] J. P. K. Doye, M. A. Miller, and D. J. Wales, *J. Chem. Phys.* **110**, 6896 (1999).
- [18] C. L. Cleveland, W. D. Luedtke, and U. Landman, *Phys. Rev. Lett.* **81**, 2036 (1998).
- [19] R. S. Berry and B. M. Smirnov, *J. Chem. Phys.* **113**, 728 (2000).
- [20] R. H. Leary and J. P. K. Doye, *Phys. Rev. E* **60**, R6320 (1999).
- [21] E. Marinari and G. Parisi, *Europhys. Lett.* **19**, 451 (1992).
- [22] J. P. K. Doye, M. A. Miller, and D. J. Wales, *J. Chem. Phys.* **111**, 8417 (1999).
- [23] J. P. Neirotti, F. Calvo, D. L. Freeman, and J. D. Doll, *J. Chem. Phys.* **112**, 10340 (2000).
- [24] D. J. Wales, *Mol. Phys.* **78**, 151 (1993).
- [25] D. J. Wales *et al.*, *Adv. Chem. Phys.* **115**, 1 (2000).
- [26] More accurate anharmonic forms are available [J. *Chem. Phys.* **102**, 9659 (1995)] but these are cumbersome and less transparent. Use of the harmonic approximation leads to an overestimation of T_{ss} , but this error is small for the examples in Table I.
- [27] M. A. van der Hoef, *J. Chem. Phys.* **113**, 8142 (2000).
- [28] A. P. Sutton and J. Chen, *Phil. Mag. Lett.* **61**, 139 (1990).
- [29] R. P. Andres *et al.*, *Science* **273**, 1690 (1996).
- [30] W. Branz, N. Malinowski, H. Schaber, and T. P.

Martin, Chem. Phys. Lett. **328**, 245 (2000). [32] B. W. van de Waal, Phys. Rev. Lett. **76**, 1083 (1996).

[31] F. Baletto, C. Mottet, and R. Ferrando, Phys. Rev. Lett. **84**, 5544 (2000).